Neuroscience, Volume 84, Issue 2, pages 603-617

Tonic and bursting activity in the cuneate nucleus of the chloralose-anesthetized cat

A. Canedo, L. Martínez, J. Mariño

Abstract
Whole-cell recordings were obtained from cuneate neurons in anesthetized, paralysed cats. Stimulation of the contralateral medial lemniscus permitted us to separate projection cells from presumed interneurons. Pericruciate motor cortex electrical stimulation inhibited postsynaptically all the projection cells (*n*=57) and excited all the presumed interneurons (*n*=29). The cuneothalamic cells showed an oscillatory and a tonic mode of activity. Membrane depolarization and primary afferent stimulation converted the oscillatory to the tonic mode. Hyperpolarizing current steps applied to projection neurons induced a depolarizing sag and bursts of conventional spikes in current-clamp records. This indicates the probable existence of low-threshold and hyperpolarization-activated inward currents. Also, the hyperpolarization induced on projection cells by motor cortex stimulation deinactivated a low-threshold conductance that led to bursting activity. The presumed cuneate interneurons had larger and more proximally located peripheral receptive fields than the cuneothalamic cells. Finally, experiments specifically designed to test whether motor cortex-induced presynaptic inhibition could be postsynaptically detected gave negative results.
These results demonstrate, for the first time, that the cuneothalamic cells possess both bursting and tonic firing modes, and that membrane depolarization, whether produced by injection of positive current or by primary afferent stimulation, converts the oscillatory into the tonic mode.

Keywords: cuneate nucleus; intracellular recording; cat

Abbreviations: CN, cuneate nucleus; DC, dorsal column; EGTA, ethyleneglycolbis(aminoethyl ether)tetra-acetate; EPSP, excitatory postsynaptic potential; HEPES, *N*-2-hydroxyethylpiperazine-*N*′-2-ethanesulfonic acid; IPSP, inhibitory postsynaptic potential; MCx, pericruciate motor cortex; ML, medial lemniscus; RF, peripheral receptive field

The cuneate nucleus (CN), in its middle part (0–4 mm caudal to the obex), is constituted by two well-differentiated zones: (i) a core or clusters region[29]that predominantly receives cutaneous input and that is rich in cuneothalamic cells; (ii) a shell. The shell consists of a ventral region in which deep input prevails, and a series of neurons in the borders of the nucleus that receive cutaneous and deep input.[17]Whereas the primary afferents terminate in the clusters region, where they synapse only on dendrites without making axosomatic synaptic contacts,[17]the descending corticocuneate axons terminate primarily in regions outside the clusters zone, where they synapse with interneurons.1 and 57The great majority of the cells in the clusters region project almost exclusively to the ventroposterolateral nucleus of the contralateral thalamus. Before entering the medial lemniscus (ML), the cuneothalamic cells emit recurrent collaterals that terminate either within the clusters region or more ventrally, but do not terminate in regions containing the dendritic arbors of the parent cuneothalamic neurons.[18]

Volitional motor commands are dependent upon sensory clues, and somesthetic signals can modify motor cortex output. Lesions of the cat's motor cortex can pass undetected when the animal walks on a planar surface, but produce major deficits when the animal performs more precise movements requiring exact placement of the foot under sensory guidance.3, 32 and 35Thus, sensory information is necessary for motor cortex function. Furthermore, the motor cortex modulates the incoming somatosensory ascendant transmission at the level of the dorsal column (DC) nuclei through two different routes:26, 31 and 33one excitatory, running in the pyramidal tract; and one inhibitory, which can follow either a pyramidal or extrapyramidal pathway.[26]Recently, it was shown that the pericruciate fibers directed to the contralateral cuneate nucleus and running in the pyramidal tract are slow conducting and tend to terminate at supraspinal and cervical cord levels.[36]Therefore, the pericruciate motor cortex (MCx)

might modify its own somatosensory inputs through pyramidal tract fibers mostly directed contralaterally to both the cervical spinal cord and the DC nuclei.

The receptive fields of cuneate cells are larger than those of primary afferent fibers,[46]indicating the existence of sensory convergent inputs over the same neurons. The cuneate neurons respond with a high-frequency burst of spikes to a single electrical stimulus, but show more spontaneous activity than their afferents and can generate bursting activity in the absence of afferent input.6 and 19Also, the majority of the thalamic-projecting neurons in the clusters region receive convergent input from multiple receptor classes.[18]These findings, together with the recent demonstration that the cuneate neurons show slow (<1 Hz) and delta (1–4 Hz) rhythms tightly coupled to the same oscillating activities recorded simultaneously in the contralateral ventroposterolateral nucleus of chloralose-anesthetized cats,[34]raise the possibility that the cuneate cells may possess an intrinsic capability to generate oscillating activity. Thus, it was hypothesized that while the slow oscillations may be imposed by the cerebral cortex,8, 34 and 51some other rhythms could be intrinsically generated.8 and 34Accordingly, the present experiments were designed to gain further information on this subject. Since cuneate neurons might present bursting and tonic modes of operation, a first concern of this work was directed to this possibility. Because of the results, a second concern of the study was primarily directed to unravel the mechanisms that would permit the change between bursting and tonic activities. To deal with these questions, intracellular recordings were obtained from cuneate neurons which were classified as cuneothalamic or presumed interneurons by strong electrical stimulation of the contralateral ML. Preliminary results have been reported in abstract form.[37]

1. Experimental procedures

1.1. General

A total of 60 cats of either sex (2.3–4.5 kg) were anesthetized (α-chloralose, 60 mg/kg, i.p.), paralysed (Pavulon, 1 mg/kg/h, i.v.) and artificially respired (ventilation adjusted to maintain end-tidal CO_2 between 4 and 4.5%). Additional doses of anesthesia were administered when necessary. The depth of anesthesia was assessed by monitoring the heart rate and by observing the state of the pupil. Changes in heart rate and dilated pupils, or pupils reacting rapidly to the electrical stimuli, were considered to reflect inadequate anesthesia, and supplementary doses of 30–40 mg/kg of α-chloralose were injected every 4–6 h, as required. Rectal temperature was maintained at 37.5±0.5°C by an abdominal heating pad under servo-control. Tracheal and venous cannulae were inserted and the animal was positioned in a stereotaxic frame with the head flexed by about 30–40° to allow easy access to the dorsal medulla. The animals were suspended with clamps attached to thoracic and lumbar vertebrae, and the most caudal cerebellum was suctioned. The dorsal medulla was exposed to insert recording electrodes within the middle main CN from the level of the obex to 4 mm caudal to it. In this region the thickness of the nucleus is maximal and most neurons project to the contralateral ML. 1, 18 and 29To minimize the respiratory and pulsatile movements, a bilateral pneumotorax was routinely carried out, and a 4% agar solution in 0.9% saline at 38°C was poured over the exposed medulla to a high of about 10 mm.

1.2. Stimulation

To identify antidromically projecting cells, a bipolar stimulating electrode (0.5 mm inter-tip space, 40–50 μm diameter and insulated except at the tip) was introduced through a craniotomy into the contralateral ML at A2. Correct placement was achieved by recording evoked potentials and multi-unitary responses to mechanical and electrical stimulation of the contralateral forelimb (see inset in Fig. 1B). A silver ball stimulating electrode was positioned over the homolateral DC at C2 to stimulate the primary afferent fibers. A set of six concentric bipolar stimulating electrodes was mounted in a tower and lowered through a craniotomy to 1.5 mm depth in the pericruciate cortex to stimulate corticocuneate fibers. Three of these electrodes were aligned (tips separation about 1 mm) mediolaterally in the precruciate cortex, from 8 to 10 mm of the mid-line; the other three electrodes were also aligned with the same parameters in the postcruciate cortex and separated by about 3 mm from the precruciate set (see Fig. 1B). Strong cathodal shocks of 0.05 ms duration and with intensities of up to 0.5 mA were applied to the ML, the center of the peripheral receptive field (RF) and to the DC at C2. Lower stimulating intensities of up to 0.2 mA were applied to the pericruciate cortex to avoid spread of current to the corona radiata. Cathodal rectangular pulses were applied either relative to an Ag–AgCl reference anode implanted subcutaneously in the lower back, between both terminals of each bipolar electrode or between different pairs of electrodes.

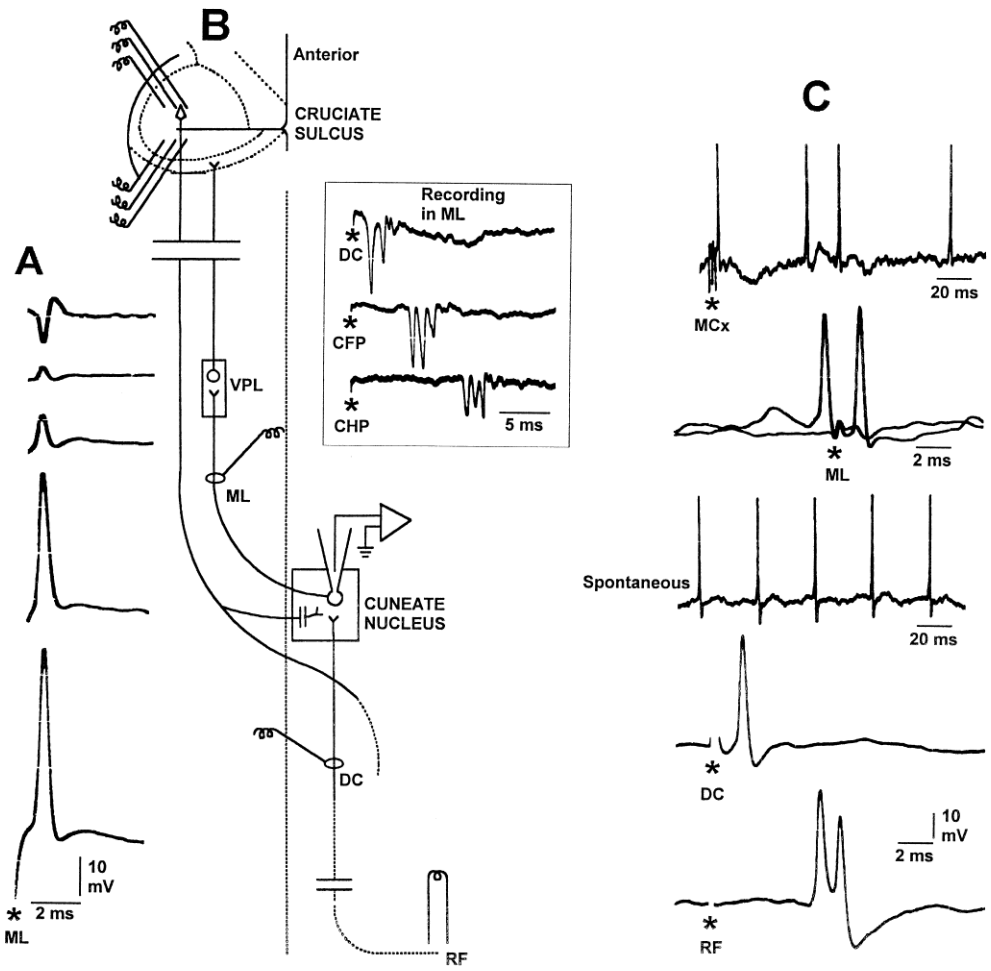

Fig. 1. Experimental procedures. (A) After a cuneate cell was extracellularly isolated whether responding to ML or to primary afferent stimulation, the micropipette was advanced until the polarity of the spike reversed. Then, gentle suction was applied to form a seal. (B) General experimental arrangement. Correct placement of the stimulating electrode in the ML was assured by averaging the field potentials evoked by dorsal column (DC), contralateral forepaw (CFP) and contralateral hindpaw (CHP) electrical stimulation (inset, 30 averaged responses). (C) A cuneate projection neuron with a rhythmic spontaneous discharge (collision between one spontaneous and one antidromically induced ML spike is shown in the second panel). Motor cortex (MCx) stimulation with a train of three pulses induced an inhibitory response (upper panel). Stimulation of the dorsal column (DC, fourth panel) and of the center of the receptive field (RF, lower panel) evoked a single and a doublet of spikes, respectively. Stimulus artifacts are marked by asterisks.

Projection cells (because most of the lemniscal fibers project to the thalamus these neurons are, with all probability, cuneothalamic cells) were identified as antidromically activated by ML stimulation according to standard criteria,9, 30 and 36including, in all cases, the collision test as well as confirmation that the critical interval in the collision was not due to soma refractoriness (e.g., second panel in Fig. 1C). This was accomplished by using double shocks to evoke paired antidromic responses separated by a delay less than the minimum interval in the collision test.

1.3. Extracellular recording

When a cell was extracellularly isolated, its RF was determined. Peripheral stimulation consisted of moving joints passively for proprioceptors, and brushing, touching or pressing skin and deeper tissues for other receptors. A narrow jet of compressed air as well as light brushing with a vibrissal hair held in a small chuck were very useful to stimulate hair receptors. In the cuneate region sampled, the cuneothalamic cells had small cutaneous receptive fields on the distal forelimb regions, and responded to low-intensity stimulating currents applied to the DC. Once the RF was determined, a pair of needle stimulating electrodes was inserted in the center of the RF. The disadvantage of non-physiological stimulation is compensated by the temporal precision of the stimulus, which permits us to have

unequivocal measure of latencies and to perform conditioning–test interactions. Next, ML stimulation was accomplished to find whether the neuron was a cuneothalamic projection cell. Thereafter, the center of the RF and the DC were stimulated, at increasing frequencies, to find the capability of the cell to follow 1:1 afferent stimuli.

1.4. Whole-cell recording

Intracellular current-clamp records were obtained using the whole-cell technique employed previously in the *in vivo* visual cortex of the cat. 14, 15, 23 and 42The electrodes were pulled from borosilicate glass (o.d. 1.5 mm, i.d. 0.85 mm) with a two-stage pull on a horizontal puller (Sutter Instruments, Novato, CA, U.S.A.). Resistance measured *in vivo* ranged from 10 to 20 MΩ, with the electrodes filled with a solution buffered to pH 7.2 containing (in mM): KCl, 20; potassium acetate, 90; $MgCl_2$, 3; $CaCl_2$, 1; HEPES, 40; EGTA, 3; GTP, 0.4; Na_2ATP, 4; biocytin, 1%. The solution was adjusted to 300 mOsm with saccharose. Before penetration into the neural tissue, the electrode was positioned over the CN using a motorized driver, the tissue was then covered with warm agar and, when solidified, the electrode was introduced and the search for cuneate neurons began.

When a cell was extracellularly isolated, its RF was determined and the antidromicity to ML stimulation tested. Electrode resistance was continuously checked by observing the change in voltage produced by current pulses (50 ms duration; −100 to −200 pA intensity) using an axoclamp-2B intracellular amplifier (Axon Instruments, Forster City, CA, U.S.A.) in the bridge mode. The bridge was balanced and the capacitance neutralization adjusted to give the fastest step response to a current pulse. Positive pressure was not applied to the micropipette since extrusion of internal solution will tend to equal the intracellular medium, which would lead to a voltage decrease of the cellular responses. Electrical stimulation to the ML and/or to the DC was applied while the electrode was advanced in 1–2 μm steps until the shape of the extracellular spike varied from negative to positive (see Fig. 1A). This procedure was particularly useful since the spike was gradually reversing polarity that could be easily followed. The reversal of the spike polarity was taken as evidence that the electrode contacted the membrane of the neuron when the resistance increased by 10–40 MΩ. Thereafter, gentle suction was applied through a small syringe to form a seal. Further pulses of negative pressure were applied to break the seal and to observe a sudden drop in the resistance, a resting potential, and synaptic potentials in response to electrical stimulation. Typical series resistances varied between 3 and 15 MΩ.

The output of the amplifier was monitored on an oscilloscope and stored in a digital tape recorder (sampling frequency per channel: 12–48 kHz) for further analysis. Also, current–voltage curves were computed by injecting intracellular current pulses of 50–300 ms duration and intensities from −1.25 to 1.25 nA in 0.25-nA steps (Fig. 3 and Fig. 5BFig. 8). The voltage responses to the injected currents were filtered at 3 kHz and stored in a 486 personal computer at a sample rate of 10 kHz for later analysis using pClamp6 software (Axon Instruments). Measurements of resting potentials were made by comparing intracellular with extracellular d.c. levels recorded on the tape.

1.5. Histology

Following histological processing,[22]we were unable to find any fully and clearly labeled neurons. The reason could be that the neurons were not maintained long enough to permit the diffusion of the biocytin and/or that the recording electrode was always intracellularly maintained until neuronal deterioration. Reconstruction of the electrode tracks revealed that the recordings were made within the middle main CN.

2. Results

2.1. General

The technique permitted stable recordings for an unusually long duration in this highly pulsating part of the brainstem (10–20 min; n=86). We focused our attention on the change of the responses in function of afferent stimuli and injection of current, more than in the absolute size of the potentials. As long as the conditions of recording are maintained constant, comparison of responses induced by afferent stimuli and injection of current should reflect the basic properties of the recorded neurons. [13]

To evaluate whether the use of Pavulon (obtained from our hospital facilities) should be avoided, the spontaneous and peripherally evoked activities of cuneate neurons were studied extracellularly in two pilot experiments. Some neuronal properties were evaluated, first in the non-paralysed animal and then

under continuous venous infusion of Pavulon or decamethonium bromide in the same animal. Since, at the systemic doses utilized (1 mg/kg per h), neither substance induced statistically significant variations in the responses of cuneate neurons to mechanical and electrical stimuli applied to the center of their RFs (threshold, mean latency, mean number of spikes, stimulating frequency-following) nor varied the size of the RFs (size, modality) in chloralose-anesthetized cats, Pavulon was subsequently used.

Strong electrical shocks applied to the contralateral ML allowed us to distinguish presumed cuneate interneurons from projection cells. Although there is always the uncertainty that lemniscal stimulation could fail to antidromically activate all the cuneothalamic cells, evidence demonstrating differential properties between projection neurons and presumed local neurons is presented that permits us to be reasonably confident when separating these two classes of cells.

Resting potential was taken as the difference between the intracellular and extracellular potentials after withdrawing the recording micropipette. Current pulses of the same amplitude as used during intracellular recording were applied to ensure the absence of artifacts that would have resulted from improper capacitance compensation or microelectrode polarization. Resting potentials for the 57 projection neurons averaged −50 mV (range: −38 to −75 mV). Their input resistances, measured with current pulses of −75 pA passed through the recording micropipette, varied from 20 to 76 MΩ (mean±S.D.: 35±14 MΩ). Resting potentials for the 29 neurons that failed to respond antidromically to ML stimulation averaged −49 mV (range: −33 to −78 mV), and their input resistances varied from 35 to 96 MΩ (41±18 MΩ). Responses to current injection were obtained during the first 1–3 min of the recording. The mean antidromic latency for the cuneate projection cells was 1.2±0.2 ms (mean±S.D.), with no significant differences related to their rostrocaudal or dorsoventral locations. These projection neurons appeared at depths between 700 and 2000 μm from the surface. The presumed interneurons appeared more superficially and more ventrally.

2.2. Peripheral receptive fields

The size of the RFs varied with the location of the fields on the skin. The smallest fields appeared on the distal parts of the forelimb. The fields became progressively larger in the proximal forelimb and trunk. There was a significant difference in field size between projection cells and presumed interneurons. The non-projection neurons had larger RFs that were located proximally in the limb and trunk. Overall, the cells fired in response to displacement of hairs (42/86 or 48.8%: 34/57 or 59.6% of the projection cells, 8/29 or 27.6% of the presumed interneurons), to light touch (28/86 or 32.5%: 18/57 or 31.5% of the projection cells, 10/29 or 34.5% of the interneurons) or pressure (10/86 or 11.6%: 5/57 or 8.8% of the projection cells, 5/29 or 17.2% of the presumed interneurons) applied to the skin. The remaining six cells (all presumed interneurons) responded to passive proprioceptive stimulation.

Manual peripheral sensory stimulation induced sustained depolarizations. While the receptive field properties were studied extracellularly for all the sampled neurons, the intracellular properties were derived from five single-spike, six bursting and two silent cuneothalamic cells. Electrical stimulation in the center of the RFs yielded more complex responses which will be reported separately, since it is necessary to delimit the different receptors and/or terminals stimulated. Fig. 2 shows examples of the extracellular responses induced in two projection neurons to light touch (Fig. 2A) and to movement of hairs (Fig. 2B) in the center of their RFs, located in both cases in the distal forelimb. The cells showed no apparent adaptation, since both responded during the whole period of stimulation (marked by horizontal bars). Interestingly, following peripheral stimulation, the cells stopped their spontaneous firing during prolonged periods of time (minutes in some cases). However, during these pauses the neurons responded very well to the stimulation of their RFs and, generally, field potential oscillations of about 4 Hz were visible extracellularly, as reported previously.[34]These oscillating field potentials probably reflected the rhythmic activity of groups or clusters of cells in close proximity. The intracellular behavior of the bursting cells to manual stimulation of their RFs is exemplified by the records of Fig. 2C and D. Fig. 2C illustrates a cuneate projection neuron that oscillated spontaneously, generating bursts of two spikes. Movement of hairs of the dorsal part of the most distal forelimb using a vibrissal hair evoked long depolarizing periods crowned by spikes of higher amplitude than in control conditions. These spikes with varying amplitudes suggest that they were generated in the dendritic arbor, and the recording electrode was probably located in a dendrite.[52]Upon cessation of peripheral stimulation, the cell remained sufficiently depolarized to disrupt its oscillating mechanism during various hundreds of milliseconds. If the RF was stimulated during the silent period that followed a previous stimulation, it again generated long depolarizations leading to high-amplitude spikes. The projection neuron shown in Fig. 2D also discharged rhythmically, generating spike doublets. Manual stimulation of the RF caused a maintained depolarization that led to tonic firing during the full stimulating period. The depolarization induced by

sensory stimulation replaced the oscillating activity by single-spike, tonic activity, very much like thalamocortical neurons.47 and 48

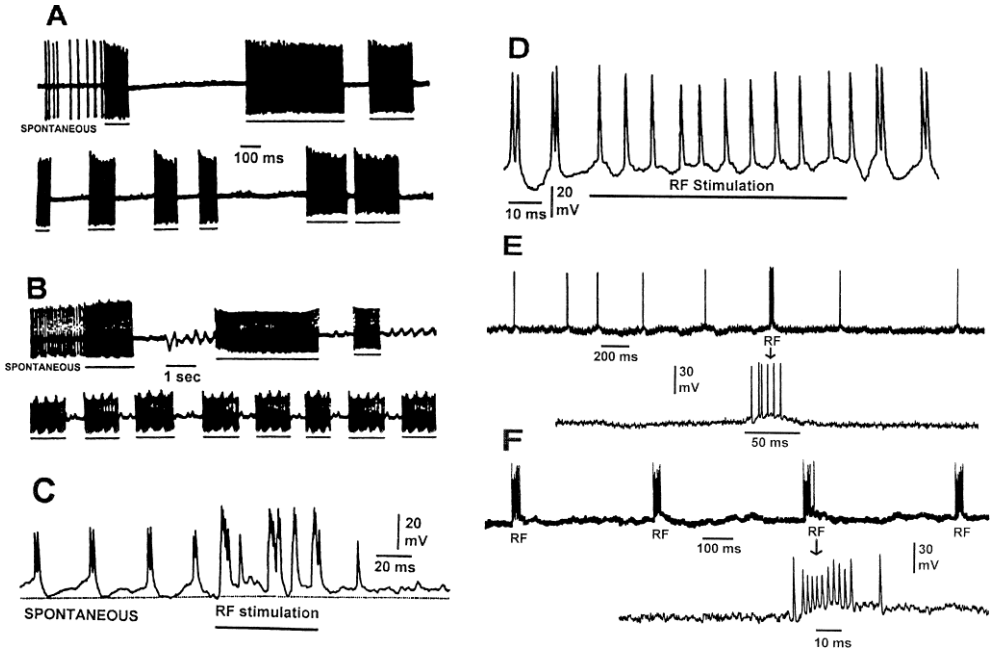

Fig. 2. Responses of projection cells to sensory afferent stimulation. Extracellular responses of two cuneothalamic neurons (A, B) to manual stimulation of their cutaneous RFs. The horizontal bars mark the stimulating periods. The intracellular responses of two different projection bursting cells (C, D) show that manual stimulation of their RFs induced membrane depolarization converting their oscillatory activity into single, tonic activity. A single-spike (E) and a silent neuron (F), both projection cells, responded to light tapping of the homolateral central forepaw with sustained depolarizations leading to the production of spikes (see the specimen records expanded below). Although the oscillatory neurons did not have a true resting potential, their more negative spontaneous excursion reached −50 mV (C) and −60 mV (D). Resting membrane potentials for the neurons shown in E and F were −50 and −55 mV, respectively.

Manual stimulation of the RFs of single-spike and silent projection cells showed, basically, a similar behavior (Fig. 2E, F). The cells responded with a sustained depolarization, leading to the generation of spikes in which, in the case of the two silent neurons, a first conventional potential was invariably followed by incomplete responses (Fig. 2F) that could reflect the partial inactivation of sodium channels or, alternatively, dendritic potentials electrotonically conducted to the soma.

2.3. Responses to afferent input

Motor cortex stimulation evoked excitatory responses in all the presumed interneurons (n=29). These responses usually reached threshold and led to propagated spikes followed by postspike hyperpolarizations and rebound depolarizations that also reached threshold in most cases (see also Ref. 8 [8]). In contrast, MCx stimulation evoked inhibitory responses in all the projection cells (n=57; Fig. 3 Fig. 5A), and injection of hyperpolarizing currents through the recording electrode reversed the polarity of the inhibitory postsynaptic potentials (IPSPs) (Fig. 3). The IPSPs evoked by MCx stimulation on the projection cells had a mean latency of 9 ms (range: 7.5–15 ms) and a duration ranging from 25 to 70 ms, with a mean of 35 ms. The excitatory postsynaptic potentials (EPSPs) evoked by MCx stimulation on the presumed interneurons had a mean latency of 5.5 ms (range: 2–10 ms) and were less sensitive to hyperpolarizing currents than the IPSPs evoked on the projection cells. The interneuronal IPSPs also reversed polarity upon injection of hyperpolarizing currents (not shown).

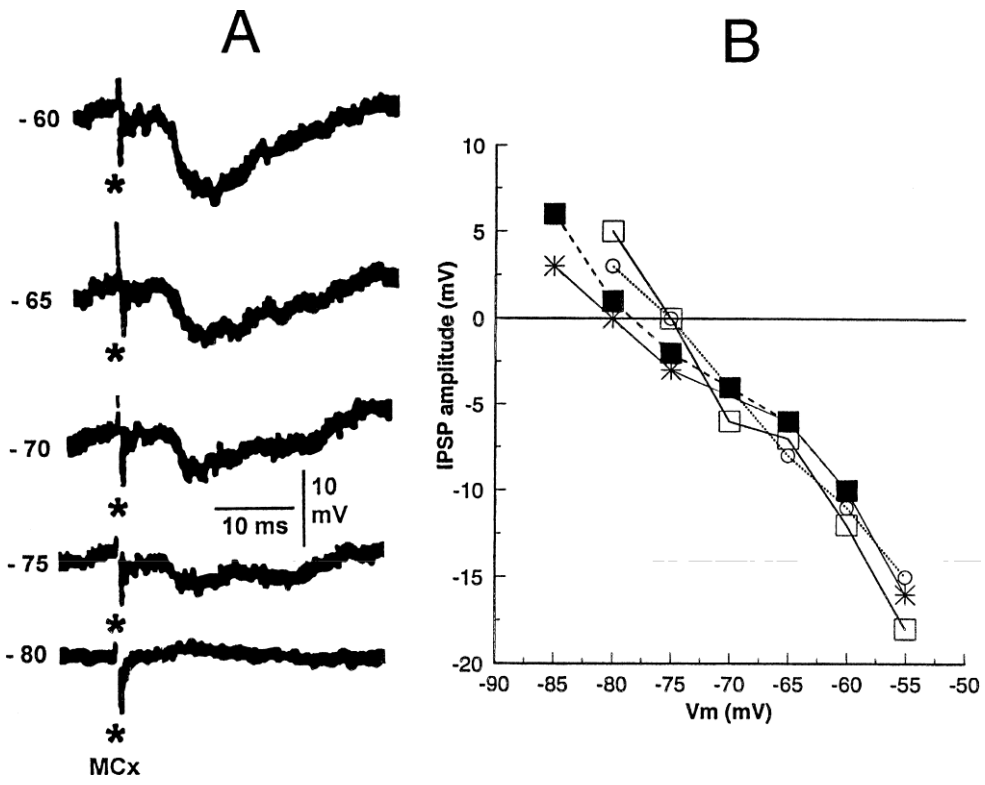

Fig. 3. MCx stimulation induced IPSPs in cuneothalamic neurons. (A) The inhibitory potential evoked in a projection neuron upon stimulation of the MCx reversed polarity at a membrane potential of about −80 mV. (B) Voltage–current plots for four different cuneothalamic cells, showing that the MCx-induced IPSPs reversed polarity at membrane potentials between −75 and −80 mV. MCx stimulus artifacts are marked by asterisks.

Primary afferent electrical stimulation in the periphery produced inhibitory (*n*=4) and excitatory (*n*=15) responses in presumed cuneate interneurons (19 tested), and a first monosynaptic excitatory response in projection cells, sometimes followed by a later hyperpolarization (37 of 37 cells tested). Bear in mind that excitatory fields were searched, extracellularly, that a bipolar needle for electrical stimulation was inserted in the center of the field, and that the stimulating current may diffuse to other receptors and/or fiber terminals. Spikes and/or EPSPs were considered to be produced monosynaptically when they were produced in a 1:1 manner following peripheral stimulating frequencies of 150 Hz or higher. While high-frequency stimuli (trains of 5–20 stimuli up to 500 Hz in some cases) applied to the DC were consistently followed by the projection cells in a 1:1 manner, the presumed interneurons (all of six tested: four single-spike and two bursting cells) failed to follow stimulating frequencies of 100 Hz or higher. One example is shown in Fig. 4, illustrating a presumed local neuron that discharged rhythmically, generating pacemaker-like potentials that led to propagated spikes at rest. Iterative stimulation of the DC at 100 Hz kept the cell partially hyperpolarized. After a variable number of successive monosynaptically evoked responses, the firing mechanism regularly failed. Consequent to stimulation, the conventional action potentials were often preceded by shorter waveforms (see the expanded lower records of Fig. 4). These partial responses appeared in isolation following each shock to the DC every time the firing mechanism failed. Thus, at least some of the presumed local cells seem to have intrinsic membrane properties restricting their capability to follow a 1:1 afferent stimulus at frequencies of 100 Hz or higher. The inability of the presumed interneurons to follow 1:1 afferent stimulation could also be explained in part by the sparser projections of the DC to the shell with respect to the clusters region.

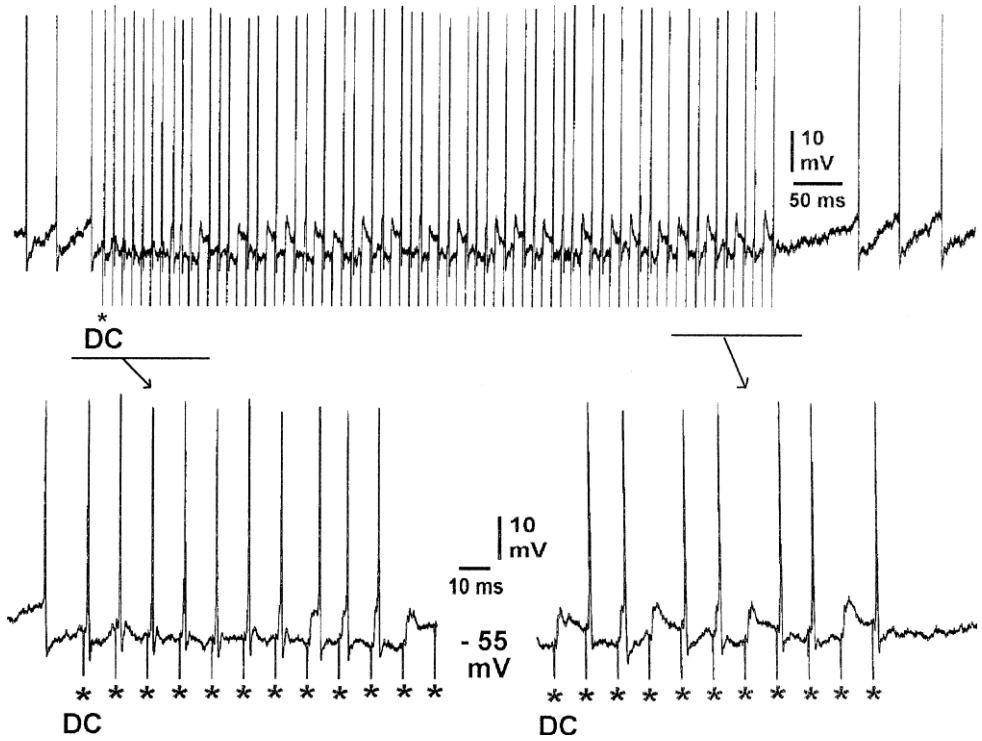

Fig. 4. The presumed interneurons did not follow high-frequency afferent stimulation. A stimulating train of 700 ms duration at 100 Hz was applied to the DC (upper panel; the first stimulus artifact is marked with an asterisk). The parts marked by horizontal lines at the beginning and end of the train are expanded below. Note that although the presumed local neuron did not follow a 1:1 stimulus, the failures were discontinuous. The short waveforms preceding the spikes were uncovered each time the DC stimuli failed to induce conventional action potentials. These short and incomplete responses represent, in all probability, postsynaptic potentials.

2.4. Rhythmic activity

In the deeply anesthetized, paralysed cat, most of the cuneate cells were spontaneously active (50/57 of the projection neurons and 25/29 of the presumed interneurons), discharging in single spikes (16/50 cuneothalamic cells and 12/25 presumed interneurons) or in bursts of two to five spikes.

The hyperpolarization induced by motor cortex stimulation generated bursting activity in 25 of 35 projection cells tested as illustrated in the example shown in Fig. 5A. Fig. 5B shows another example in which hyperpolarization from rest (−55 mV) of the projection cell gradually increased the appearance of a low-threshold potential that led to the generation of bursts of conventional spikes. Membrane depolarization from hyperpolarized values gradually decreased this low-threshold potential, which was canceled at depolarized values from rest, although some burst discharges were still present. This indicates that the tendency of cuneothalamic cells to generate repetitive firing might be sustained by different mechanisms. Furthermore, depolarization from rest showed that the amplitude of the fast postspike hyperpolarization increased gradually, demonstrating its voltage dependence. Also, injection of depolarizing currents converted the spontaneous bursting activity of projection cells (12 of 12 tested; Fig. 5C) and presumed interneurons (five of five tested) into single-spike, tonic discharges.

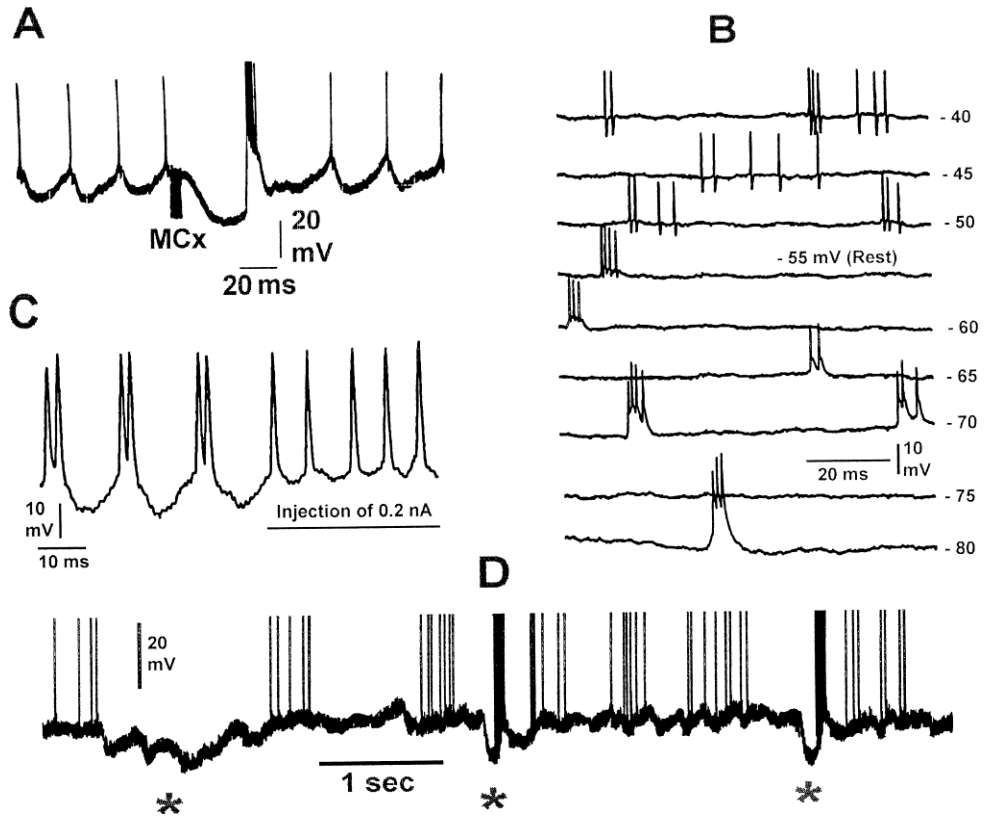

Fig. 5. Responses of projection cells to membrane polarization. (A–C) Three different cuneothalamic neurons. The cell shown in A responded to a high-frequency train (600 Hz) of six electrical stimuli applied to the tip of the cruciate sulcus (MCx), generating an inhibitory response that, in turn, induced bursting activity, probably by deinactivating a low-threshold conductance. Intracellular injection of current in the neuron illustrated in B demonstrated that different conductances were activated at distinct membrane potentials. While hyperpolarization induced bursting activity, depolarization led to single, tonic discharges, with the fast postspike hyperpolarization decreasing in amplitude with the degree of depolarization. The neuron illustrated in D showed spontaneous membrane rhythms within the range of delta (1–4 Hz) and slow (<1 Hz, asterisks) oscillations. The spikes in D are truncated. During spontaneous activity the intracellular membrane potentials reached maxima of −57 mV (A), −55 mV (B), −58 mV (C) and −60 mV (D).

In addition, both projection cells and presumed interneurons presented resting rhythmicites, including slow[34](<1 Hz; Fig. 5D), delta (1–4 Hz) and gamma (30–80 Hz; Fig. 6) oscillations. Particularly, the hyperpolarizations leading to slow oscillations were very prominent (range: 10–23 mV; from eight projection neurons and five presumed interneurons; no significant difference for both classes of cells) and sometimes delta-like oscillations appeared during the hyperpolarizing periods (Fig. 5D, asterisk at left). These slow hyperpolarizations usually led to the generation of bursting activity (Fig. 5D, two asterisks at right). The rhythmicity of single-spike discharging cells was also voltage dependent. Within the range of 25 mV, the increase in the number of spikes was approximately linear with membrane depolarization both for presumed interneurons (n=5) and projection cells (n=6) (Fig. 6). On average, the interneurons appeared to be slightly more sensitive to membrane depolarization. Depolarization exceeding 25 mV from rest usually led to neuronal deterioration (the cell illustrated in the upper panel of Fig. 6 was the only exception) and was not taken into account for analysis.

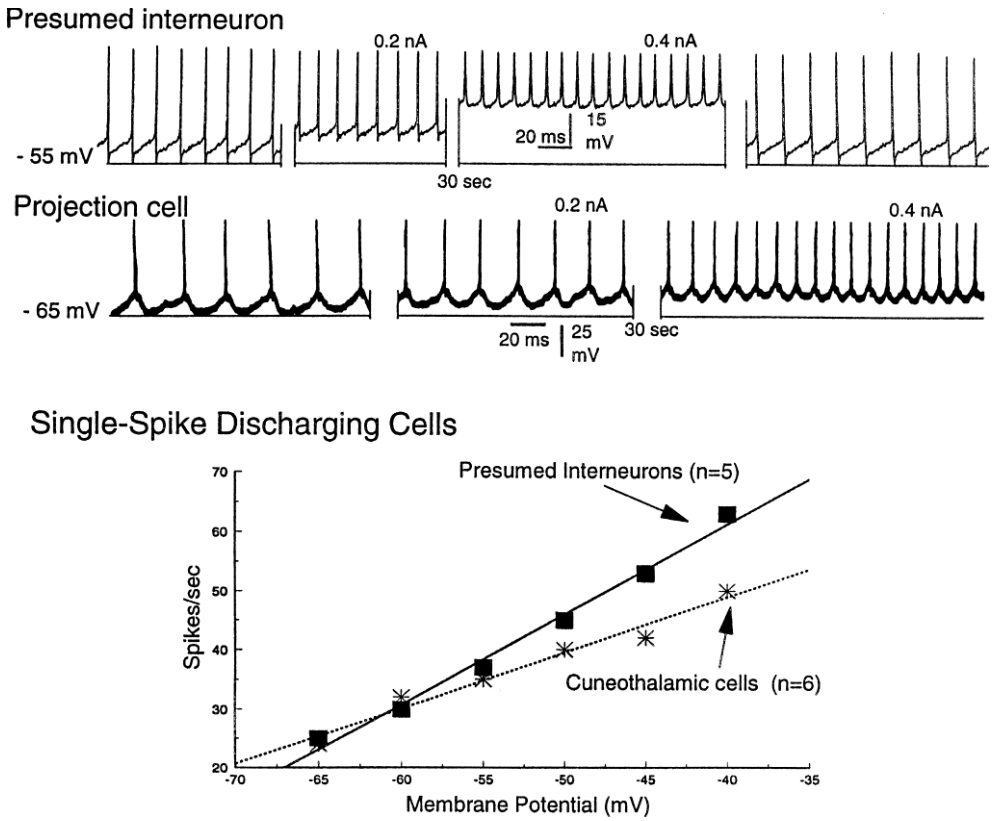

Fig. 6. Effect of membrane potential on the firing frequency of cuneate neurons. Injection of depolarizing current pulses induced increases of firing frequency in a presumed interneuron (top panel) and in a projection cell (middle panel). Each of the first two panels show the resting activity at left (and also at right in the upper panel), and then the effects of successive current injections of 0.2 and 0.4 nA, separated by periods of 30 s for neuronal recovery. The lower panel graphically illustrates the mean increases of frequency in function of the membrane potential for the 11 neurons tested, within the range of 25 mV. Voltage calibration is valid for A–C.

In summary, the voltage dependence of single-spike versus bursting activity is apparent even when dealing with undershooting records. Furthermore, the rhythmic discharges are not due to intracellular impalement, since they are also observed in extracellular records (Fig. 7; also see Ref. 34). Thus, it appears that cuneothalamic neurons do possess intrinsic membrane properties, allowing them to change from bursting to tonic activity.

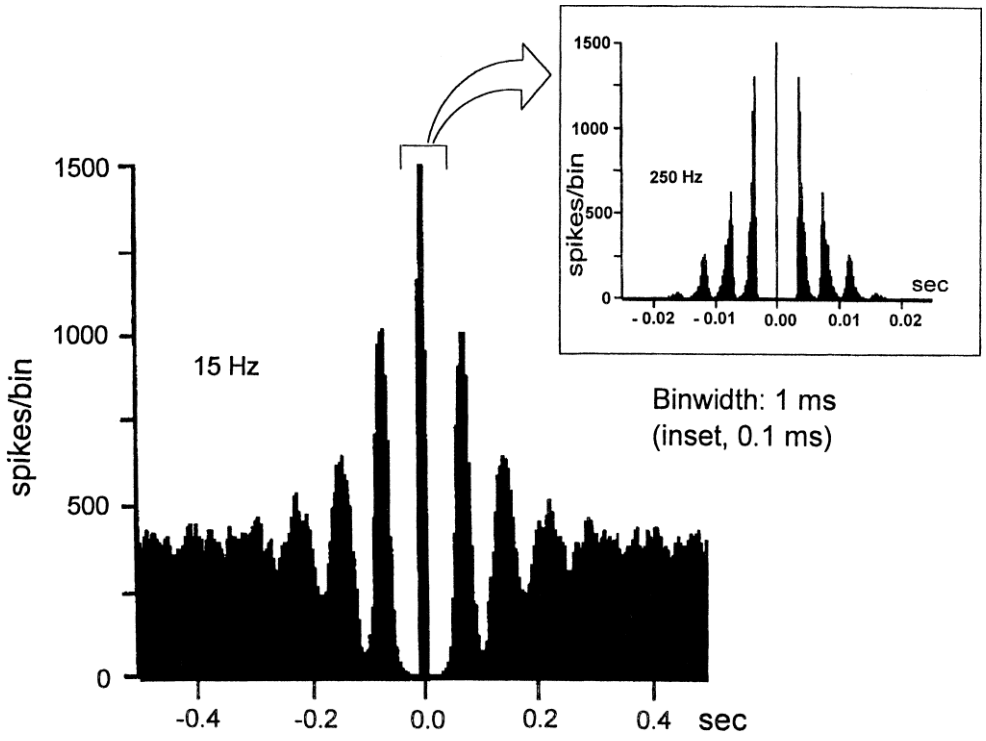

Fig. 7. The rhythmic activity was not impalement dependent. Autocorrelograms from a cuneate projection neuron computed with bins of 1 ms (left) and 0.1 ms (inset) are shown. Detected events were the neuronal extracellular spikes. The histogram in the inset represents the expanded portion marked by the bracket on the left of the autocorrelogram.

2.5. Low-threshold and hyperpolarization-activated responses

It is well known that thalamocortical neurons generate rhythmic oscillations through the interaction of a slow inward rectifier current (I_H) and a low-threshold calcium current (I_T). 38, 39, 41 and 49If the cuneate cells possess a similar mechanism, then hyperpolarization of their membranes should activate I_H, if present, and lead to a depolarizing sag in current-clamp records. In addition, the depolarization induced by activation of I_H might eventually reach the threshold of I_T, if present, which, in turn, will trigger conventional spikes. A total of eight projection cells and six presumed interneurons were tested. Hyperpolarizing current steps from rest uncovered a depolarizing sag in all eight cuneothalamic neurons but in none of the six presumed interneurons. Fig. 8A illustrates a cuneothalamic cell that responded to DC stimulation by generating a doublet of spikes followed by a postspike hyperpolarization that led to a rebound slow depolarizing potential (probably by activation of I_T; arrow). It reached threshold and generated a conventional spike followed by a smaller postspike hyperpolarization and a subthreshold rebound depolarization at rest (Fig. 8A, black dot in left panel). When the same neuron was hyperpolarized to −75 mV from rest, the postspike hyperpolarization induced by DC stimulation decreased in amplitude, indicating its voltage dependence. A slow rebound depolarizing potential was still generated but, probably because of the underlying hyperpolarization, it was partially counterbalanced and did not reach the threshold of conventional spikes (Fig. 8A, arrow in right panel). Upon decline of the rebound potential (probably by inactivation of I_T), a slow rising repolarization (probably by activation of I_H) further led to a slow depolarizing waveform (probably by reactivation of I_T) that reached threshold (black dot in Fig. 8A, right panel) and generated a full spike. Fig. 8B shows that hyperpolarizing current pulses of 300 ms duration applied to a different cuneothalamic neuron uncovered a depolarizing sag (probably reflecting I_H) in the electrotonic potential. Upon cessation of the higher hyperpolarizing pulse, the cell generated a slow rebound potential (presumably by activation of I_T) that triggered a doublet of full spikes. The voltage responses to injected currents are shown in Fig. 8D at the peak (black dots) and 250 ms from the beginning of the injection (squares). Inward rectification occurred at membrane potentials negative to −60 mV. Series of injection currents from −1.25 to 1.25 nA in steps of 0.25 nA from rest were applied to six presumed interneurons. All six cells generated conventional spikes at the beginning and end of the depolarizing and hyperpolarizing pulses, respectively (Fig. 8C). In contrast to

the projection cells, the hyperpolarization did not uncover a depolarizing sag in the interneuronal electrotonic potential.

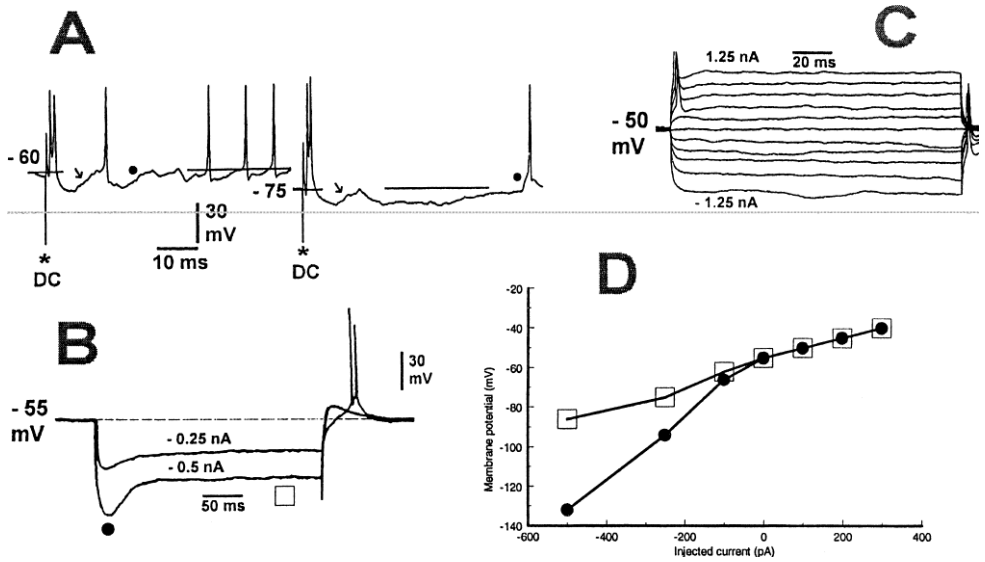

Fig. 8. Responses to current injection. Responses of two different projection neurons (A, B) and of a presumed interneuron (C) to injection of current through the recording electrode. The cell illustrated in A showed a rebound depolarization (arrow, left) following the postspike hyperpolarization induced by DC stimulation and that reached threshold. The subsequent postspike rebound depolarization did not reach threshold (black dot, left panel). When the cell was hyperpolarized to −75 mV from rest, the postspike rebound potential did not reach threshold (arrow, right panel) and there was a slow repolarization towards rest following the decline of the rebound potential. This repolarization induced a further slow depolarization (black dot, right panel) that reached threshold. DC stimulus artifacts are marked with asterisks. (B) Hyperpolarizing pulses of 300 ms duration uncovered a depolarizing sag in a different projection neuron. The voltages at the peak (black dot) and 250 ms after the injection (square) are compared in the plots in D. (C) Polarizing pulse steps of 150 ms duration applied to a presumed interneuron induced full spikes at the beginning of depolarizing pulses and at the end of hyperpolarizing pulses. This neuron showed a strong accommodation, but a depolarizing sag was absent in the electrotonic hyperpolarized potentials.

Thus, these data, together with results such as those illustrated in Fig. 5, point to the existence of a low-threshold conductance (presumably I_T) in projection cells and also probably in interneurons, and to a hyperpolarization-activated inward current (probably I_H) in cuneothalamic cells.

2.6. Conditioning–test interactions

It was suggested that cortical stimulation depolarized, through intranuclear interneurons, the terminals of the cuneate primary afferent fibers leading to primary afferent depolarization that, in turn, will induce presynaptic inhibition.1 and 2Since a decrease in the postsynaptic response with no accompanying membrane potential changes is an indication of presynaptic inhibition,10 and 16we searched for such a decrease in cuneate neurons in response to both motor cortex and primary afferent stimulation by using conditioning test stimuli (Fig. 9). Since it was reported that sensorimotor cortex conditioning volleys produced a maximal increase in excitability of the cuneate tract fibers to cutaneous test stimuli at inter-stimulus intervals of 40–50 ms,[1]we expected to detect a significant reduction in the amplitude of the EPSPs at similar intervals. However, as illustrated in Fig. 9, the MCx conditioning stimuli did not reduce the test cutaneous EPSPs. Postsynaptic interactions, including occlusion, were seen at reduced inter-stimulus intervals (4–19 ms). This behavior was characteristic of both projection cells and presumed interneurons (six projection cells and four interneurons tested). Thus, presynaptic effects were not postsynaptically measurable, in our hands, when MCx–RF conditioning–test stimuli were applied at different intervals. Therefore, the technique apparently did not reveal presynaptic effects, and this issue is actually under study in our laboratory, using a more specific approach trying to conclusively determine whether or not cortical afferents induce presynaptic inhibition within the CN. The failure to reduce EPSPs and firing by MCx stimulation could alternatively be due to the powerful sensory stimulation, making presynaptic inhibition difficult to detect.

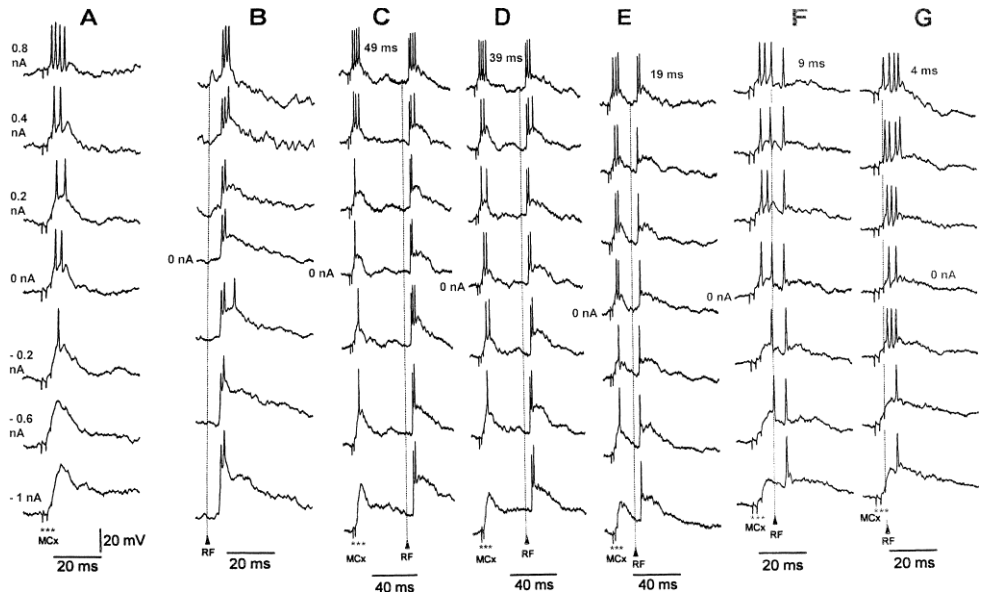

Fig. 9. Conditioning–test interactions. Each panel illustrates the responses of the same presumed interneuron to stimulation of the MCx and to electrical stimulation in the center of its cutaneous RF, both in isolation (A, B) and at different inter-stimulus intervals (indicated by the numbers given at the top of C–G). The neuron was hyperpolarized from rest (0 nA; −47 mV) and then depolarized by intracellular injection of current from −1 to 0.8 nA in steps of 0.4 nA. The recordings were taken successively from A–G during the first 11 min after impalement, which explains the gradual and parallel decrease in amplitude of the synaptically evoked responses. Stimulus artifacts are marked by asterisks (MCx) and arrowheads (RF).

3. Discussion

Some of the records show undershooting action potentials. This could reflect an incomplete seal, leading to current leakage. However, the postsynaptic responses were well recognized, the action potentials were monophasic positive with standard duration, the firing threshold was relatively constant during the recording period, and injection of current induced the typical polarity-dependent effects. In spite of the absolute size of the action potentials, the technique seems to be the most appropriate, to date, to study highly pulsating structures such as the CN. Furthermore, many of the records were similar to those obtained with sharp electrodes from other structures, and the neuronal properties described in this study did not appear to vary either in function of the absolute size of the action potentials or within the reported range of the resting membrane potentials. Also, the accepted general properties of cuneate cells are based upon intracellular recordings showing low values of membrane potentials (−20 to −30 mV), as well as undershooting spikes.[2]

Curare derivatives released microiontophoretically (flaxedil, tubocurarine) increase the firing of most cuneate neurons (mostly inducing relatively prolonged bursts rather than doublets), while microiontophoretic ejection of succinylcholine, a depolarizing neuromuscular blocker, does not affect cuneate activity.[19]However, the changes induced over cuneate cells by systemic injection of flaxedil boluses were observed with much higher doses (6–10 mg/kg/h)[19]than those necessary to induce neuromuscular blocking. Also, similar systemic doses of curare derivatives to those utilized in the present study, as well as depolarizing neuromuscular blockers, have previously been used indistinctly, without any apparent influence over the normal behavior of DC nuclei cells in both barbiturate- and chloralose-anesthetized cats.53 and 54

Although general anesthetics potentiate synaptic inhibition and depress excitatory synaptic transmission,[27]the study of corticofugal-induced effects over cuneothalamic cells precluded the decerebrate preparation. Barbiturates tend to lower terminal excitability[28]and enhance oscillatory activity,[21]while chloralose appears to increase the excitability of primary afferent terminals in the spinal cord.[7]Although pentobarbital and condensation of glucose with chloral (α-chloralose) are widely used for experimental anesthesia, their direct electrophysiological actions at anesthetic concentrations are unknown. Chloralose was the anesthetic of choice because, contrary to pentobarbital, it does not induce direct electrophysiological effects on papillary muscle action potentials [40]and preserves vagal and baroreceptor reflexes, [20]as well as the functional–metabolic coupling in the somatosensory cerebral

cortex. [55]Furthermore, the behavior of cuneate neurons has been shown to be basically the same when using chloralose, barbiturate (nembutal) and non-anesthetized, decerebrate cats. 1, 5 and 25

Because of the difficulty of maintaining a long and stable intracellular recording, pharmacological techniques were not feasible. However, the technique revealed that cuneate neurons possess bursting and tonic firing modes, and oscillatory rhythms (also see Ref. 8). The change from the oscillatory to the tonic mode is produced by membrane depolarization (Fig. 2C, D, Fig. 5), which seems to depend on afferent activity (Fig. 2C, D). If the cortex transfers its rhythmical patterns to the cuneate, then the cuneate cells must present oscillating rhythms similar to those seen in the corticothalamic network.[51]Recent data obtained in our laboratory indicate that this may be the case.[34]Since the majority of the motor cortical fibers directed to the DC nuclei are slow conducting,[36]which tend to be tonically active,[12]it is to be expected that the motor cortex inhibition and disinhibition[8]over the cuneothalamic cells would also be of a tonic nature in the non-anesthetized animal. These tonic effects could serve to differentially filter the signals incapable of overcoming the underlying inhibition, while allowing others (through disinhibition[8]) to be transmitted to the thalamus.

Since neighboring cuneothalamic cells have very similar antidromic conduction velocities,[8]their recurrent collaterals could serve to synchronize groups of nearby projection cells while, through inhibitory interneurons, inhibiting others located more distantly. Thus, inputs that may control the excitability level of the projection cells will not only influence their frequency of discharge, but also their degree of synchronization. Therefore, it could be expected that the tonic corticofugal inhibition on the cuneothalamic neurons would make their RFs simultaneously less sensitive and more discrete. Some of the motor cortical fibers directed to the DC nuclei originate from collaterals of corticospinal neurons in the cat11, 36 and 45and monkey,4 and 24but the majority (68%) derive from pyramidal tract non-corticospinal cells, at least in the cat.[36]Since about 72% of the corticospinal cells that send collateral branches to the DC nuclei terminate in the cervical cord in the cat,[36]it is probable that they are mainly engaged in the selection of ascending sensory information from the forelimbs and/or in the filtering of sensory inputs implicated in forelimb–neck–shoulder movement synergies.

The failure of presumed cuneate interneurons to follow a 1:1 afferent stimulus (Fig. 4) can be explained if these cells have calcium-activated potassium currents: $K_{(IAHP)}$. Each action potential will introduce calcium into the cell, but because this calcium will be insufficient to open the I_{AHP} channels, the cell will continue to generate spikes until there is enough calcium to open the calcium-dependent potassium channels. Consequently, the following stimulus will fail to produce a propagated response. Each silence will give sufficient time to eliminate the excess of calcium and, subsequently, the cell will respond to a few stimuli until the internal calcium rises again, beginning a new cycle. The biophysical and electrophysiological properties of the cuneate neurons are still unknown, but in analogy with thalamic neurons, where the I_{AHP} channels are amply represented and produce a similar spike-frequency adaptation, they might well have a similar behavior. Extracellularly, the intrinsic spike-frequency adaptation could be interpreted as presynaptic inhibition, which could also occur, but which we were unable to demonstrate postsynaptically (also see the conditioning–test interactions of Fig. 9). Thus, even if the presynaptic fibers release sufficient neurotransmitter (as indicated by the amplitude of the EPSPs shown in Fig. 4 and Fig. 9), and hence in the absence of presynaptic inhibition, the cuneate neurons can still select their proper frequencies of response due to their intrinsic membrane properties. If we recall that DC nuclei neurons show more spontaneous activity than their afferents and may produce spike bursts in the absence of afferent input, 6, 19 and 44this suggests that this activity might be due to intrinsic membrane properties. There is the possibility that chloralose may suppress the cortically induced presynaptic inhibition, but different authors have claimed, based on extracellular recordings, the existence of presynaptic inhibition in chloralose-anesthetized cats, 5, 7 and 25including presumed primary afferent depolarization of cuneate tract fibers. [5]If presynaptic inhibition is due to axoaxonic synapses of GABAergic cuneate local neurons over primary afferent terminals, and since stimulation of the motor cortex activates the interneurons, the presynaptic inhibition should be detectable postsynaptically. However, motor cortex stimulation did not reduce the size of the EPSPs, which indicates that either the technique is not appropriate to study presynaptic effects or that presynaptic inhibition did not take place in our sampled cells.

The cuneate inhibitory interneurons may diminish sensory transmission by increasing the inhibition over cuneothalamic cells. Inhibition of these interneurons (disinhibition) may increase the sensory transmission through the cuneate.[8]However, the intrinsic properties alone do not explain the selective choice of wanted from unwanted sensory transmission. In particular, wired networks are also necessary. There might be a somatotopical arrangement based upon the assumption that neighboring cuneothalamic neurons have similar RFs, that they project to neighboring thalamocortical cells which, in turn, activate clusters of corticocuneate neurons. In this way, the cortex could discriminate wanted from unwanted sensory information at the level of the CN by specifically producing inhibition and disinhibition over

distinct sets of cuneothalamic cells. Interneurons with differentiated characteristics have, in fact, been described in the rat CN.[56]Furthermore, the same neurotransmitter can be associated with different postsynaptic receptors and thus induce functionally distinct postsynaptic responses.[43]

Stimulation of the RFs produced exclusively excitatory responses on projection cells, which appears to be in contradiction with the results of Andersen *et al*. [2]However, while in the present study the excitatory RFs were delimited for every neuron, in the study of Andersen *et al*. [2]the ulnar and median nerves were stimulated electrically, and when inhibitory responses were seen, adjusting the intensity of stimulation also led to EPSPs and spikes that masked the IPSPs. Thus, while Andersen *et al*. [2]stimulated fibers that probably originated from the "off" and "on" peripheral receptive foci, the results described here derive from stimulation of the peripheral "on" focus.

Slow (<1 Hz) and delta (1–4 Hz) oscillatory rhythms have been detected previously in extracellular unit and field potential recordings from cuneothalamic cells.[34]While low-frequency rhythms appear to originate in the cortex, are transmitted down to the thalamus[51]and probably also to the cuneate,[34]the delta thalamic oscillations have been demonstrated to be caused by the interplay of I_H and I_T. [50]The delta cuneate oscillations could also operate via a similar mechanism. Although conclusive demonstration of these currents will require pharmacological manipulation through *in vitro* experiments, hyperpolarizing pulses appeared to uncover I_H (Fig. 8A, B, D). Furthermore, the depolarization induced by sensory stimulation inactivated a low-threshold conductance (probably I_T), allowing the cuneothalamic neurons to replace their oscillatory activity by single-spike, tonic activity (Fig. 2D). Also, hyperpolarization (Fig. 5B, D) and MCx-induced IPSPs (Fig. 5A) deinactivated this low-threshold conductance. Thus, while the cuneate slow rhythms are probably induced by corticofugal pathways, other oscillations are presumably due to intrinsic mechanisms, and those periodic rhythmicities transmitted to the thalamus may be potentiated through the intranuclear recurrent collaterals of cuneate projection neurons. [8]

4. Conclusions

In this report new data are presented on the basic properties of cuneate neurons. The results show (i) that the motor cortex stimulation induces differential effects over cuneate neurons (presumed interneurons are excited and projection cells are inhibited), (ii) that the cuneate cells have two functional modes of operation (oscillatory and tonic), thus suggesting that this dichotomy may also be valid in relay stations anterior to the thalamus and that may influence the activity of thalamic ventroposterior cells, and (iii) that there are differential RF properties between presumed local circuit neurons and cuneothalamic cells, with the former having larger RFs located proximally in the limbs and trunk.

Acknowledgements

The authors are most indebted to Dr J. Hirsch of the Rockefeller University for help in setting up the whole-cell technique *in vivo*. The criticism, helpful comments and counsel of Dr J. M. Alonso are especially appreciated. Dr J. A. Lamas critically read an earlier version of the manuscript and made many helpful suggestions. J. Mariño was a predoctoral fellow of the Xunta de Galicia. This work was supported by DGICYT (grant PB93-0345).

References

1. P Andersen, J.C Eccles, R.F Schmidt, T Yokota. Depolarisation of presynaptic fibres in the cuneate nucleus. J. Neurophysiol., 27 (1964), pp. 92–106
2. P Andersen, J.C Eccles, T Oshima, R.F Schmidt. Mechanims of synaptic transmission in the cuneate nucleus. J. Neurophysiol., 27 (1964), pp. 1096–1116
3. I.N Beloozerova, M.G Sirota. The role of the motor cortex in the control of accuracy of locomotor movements in the cat. J. Physiol., Lond., 461 (1993), pp. 1–25
4. M Bentivoglio, A Rustioni. Corticospinal neurones with branching axons to the dorsal column nuclei in the monkey. J. comp. Neurol., 253 (1986), pp. 260–276
5. M.B Bromberg, P Blum, D Whitehorn. Quantitative characteristics of inhibition in the cuneate nucleus of the cat. Expl Neurol., 48 (1975), pp. 37–56
6. A.G Brown, G Gordon, R.H Kay. A study of single axons in the cat's medial lemniscus. J. Physiol., Lond., 236 (1974), pp. 225–246
7. I Calma, A.A Quayle. Supraspinal control of the presynaptic effects of forepaw and hindpaw skin stimulation in the cat under chloralose anesthesia. Brain Res., 33 (1971), pp. 101–114

8. A Canedo. Primary motor cortex influences on the descending and ascending systems. Prog. Neurobiol., 51 (1997), pp. 287–335
9. A Canedo, J.A Lamas. Pyramidal and corticospinal synaptic effects over reticulospinal neurones in the cat. J. Physiol., Lond., 463 (1993), pp. 475–489
10. J.C Eccles, R.M Eccles, F Magni. Central inhibitory action attributable to presynaptic depolarisation produced by muscle afferent volleys. J. Physiol., Lond., 159 (1961), pp. 147–166
11. K Endo, T Araki, N Yagi. The distribution and pattern of axon branching of pyramidal tract cells. Brain Res., 57 (1973), pp. 484–491
12. E.V Evarts. Relation of discharge frequency to conduction velocity in pyramidal tract neurons. J. Neurophysiol., 28 (1965), pp. 216–228
13. D Ferster. Orientation selectivity of synaptic potentials in neurones of cat primary visual cortex. J. Neurosci., 6 (1986), pp. 1284–1301
14. D Ferster, B Jagadeesh. EPSP–IPSP interactions in cat visual cortex studied with *in vivo* whole-cell patch recording. J. Neurosci., 12 (1992), pp. 1262–1274
15. D Ferster, C Sooyoung, H Wheat. Orientation selectivity of thalamic input to simple cells of cat visual cortex. Nature, 380 (1996), pp. 249–252
16. K Frank, M.G.F Fuortes. Presynaptic and postsynaptic inhibition of monosynaptic reflexes. Fedn Proc., 16 (1957), pp. 39–40
17. R.E.W Fyffe, S.S Cheema, A Rustioni. Intracellular staining study of the feline cuneate nucleus. I. Terminal patterns of primary afferent fibres. J. Neurophysiol., 56 (1986), pp. 1268–1283
18. R.E.W Fyffe, S.S Cheema, A.R Light, A Rustioni. Intracellular staining study of the feline cuneate nucleus. II. Thalamic projecting neurons. J. Neurophysiol., 56 (1986), pp. 1284–1296
19. A Galindo, K Krnjevic, S Schwartz. Patterns of firing in cuneate neurones and some effects of Flaxedil. Expl Brain Res., 5 (1968), pp. 87–101
20. R Grad, M.L Witten, S.F Quan, D.H McKelvie, R.J Lemen. Intravenous chloralose is a safe anesthetic for longitudinal use in beagle puppies., Lab. Anim. Sci., 38 (1988), pp. 422–425
21. G.W Harding, R.M Stogsdill, A.L Towe. Comparison between neuronal samples from the pericruciate and precoronal cerebral cortex of chloralose- and barbiturate-anesthetized cats. Soc. Neurosci. Abstr., 3 (1977), p. 483
22. J.A Hirsch. Synaptic integration in layer IV of the ferret striate cortex. J. Physiol., Lond., 483 (1995), pp. 183–199
23. J.A Hirsch, J.M Alonso, R.C Reid. Visually evoked calcium action potentials in cat striate cortex. Nature, 378 (1995), pp. 612–616
24. D.R Humphrey, W.S Corrie. Properties of pyramidal tract neurone system within a functionally defined subregion of primate motor cortex. J. Neurophysiol., 41 (1978), pp. 216–243
25. S.J Jabbur, N.R Banna. Widespread cutaneous inhibition in dorsal column nuclei. J. Neurophysiol., 33 (1970), pp. 616–624
26. S.J Jabbur, A.L Towe. Cortical excitation of neurons in dorsal column nuclei of cat, including an analysis of pathways. J. Neurophysiol., 24 (1961), pp. 499–509
27. K Krnjevic. Cellular and synaptic actions of general anaesthetics. Gen. Pharmac., 23 (1992), pp. 965–975
28. K Krnjevic, M.E Morris. Input–output relation of transmission through cuneate nucleus. J. Physiol., Lond., 257 (1976), pp. 791–815
29. H.G.J.M Kuypers, J.D Tuerk. The distribution of the cortical fibres within the nuclei cuneatus and gracilis in the cat. J. Anat., Lond., 98 (1964), pp. 143–162
30. J.A Lamas, L Martinez, A Canedo. Pericruciate fibres to the red nucleus and to the medial reticular formation. Neuroscience, 62 (1994), pp. 115–124
31. M Levitt, M Carreras, C.N Liu, W.W Chambers. Pyramidal and extrapyramidal modulation of somatosensory activity in gracile and cuneate nuclei. Archs ital. Biol., 102 (1964), pp. 197–229
32. E.G.T Liddell, C.G Phillips. Pyramidal section in the cat. Brain, 67 (1944), pp. 1–9
33. F Magni, R Melzack, G Moruzzi, C.J Smith. Direct pyramidal influences on the dorsal column nuclei. Archs ital. Biol., 102 (1959), pp. 418–433
34. J Mariño, L Martinez, A Canedo. Coupled slow and delta oscillations between cuneothalamic and thalamocortical neurones in the chloralose anesthetized cat. Neurosci. Lett., 219 (1996), pp. 107–110
35. D.E Marple-Horvat, A.J Amos, D.M Armstrong, J.M Criado. Changes in the discharge patterns of cat motor cortex neurones during unexpected perturbations of ongoing locomotion. J. Physiol., Lond., 462 (1993), pp. 87–113
36. L Martinez, J.A Lamas, A Canedo. Pyramidal tract and corticospinal neurones with branching axons to the dorsal column nuclei of the cat. Neuroscience, 68 (1995), pp. 195–206

37. L Martinez, J Mariño, A Canedo. Postsynaptic effects produced by motor cortex and primary afferent fibres in the cuneate nucleus of the cat. Soc. Neurosci. Abstr., 22 (1996), p. 101
38. D.A McCormick, J.R Huguenard. A model of the electrophysiological properties of thalamocortical relay neurons. J. Neurophysiol., 68 (1992), pp. 1384–1400
39. D.A McCormick, H.-C Pape. Properties of a hyperpolarisation-activated cation current and its role in rhythmic oscillation in thalamic relay neurons. J. Physiol., Lond., 431 (1990), pp. 291–318
40. S Nattel, Z.G Wang, C Matthews. Direct electrophysiological actions of pentobarbital at concentrations achieved during general anesthesia. Am. J. Physiol., 259 (1990), pp. H1743–1751
41. H.-C Pape. Queer current and pacemaker: the hyperpolarization-activated cation current in neurons. A. Rev. Physiol., 58 (1996), pp. 299–327
42. X Pei, M Volgushev, T.R Vidyasagar, O.D Creutzfeldt. Whole cell recording and conductance measurements in cat visual cortex *in vivo*. NeuroReport, 2 (1991), pp. 485–488
43. A Popratiloff, R.J Weinberg, A Rustioni. AMPA receptor subunits underlying terminals of fine-caliber primary afferent fibres. J. Neurosci., 16 (1996), pp. 3363–3372
44. B.H Pubols Jr, J.H Haring, M.J Rowinski. Patterns of resting discharge in neurones of the racoon main cuneate nucleus. J. Neurophysiol., 61 (1989), pp. 1131–1141
45. A Rustioni, N.L Hayes. Corticospinal tract collaterals to the dorsal column nuclei of cats. Expl Brain Res., 43 (1981), pp. 237–245
46. Rustioni A. and Weinberg R. J. (1989) The somatosensory system. In *Handbook of Clinical Neuroanatomy*: *Integrated Systems of the CNS*, Part II (eds Björklund A., Hökfelt T. and Swanson L. W.), Vol. 7, pp. 219–320. Elsevier, Amsterdam.
47. M Steriade, M Deschênes. The thalamus as a neuronal oscillator. Brain Res. Rev., 8 (1984), pp. 1–63
48. M Steriade, R Llinás. The functional states of the thalamus and the associated neuronal interplay. Physiol. Rev., 68 (1988), pp. 649–742
49. M Steriade, R Curró Dossi, A Núñez. Network modulation of a slow intrinsic oscillation of cat thalamocortical neurones implicated in sleep delta waves: cortical potentiation and brainstem suppression. J. Neurosci., 11 (1991), pp. 3200–3217
50. M Steriade, D.A McCormick, T.J Sejnowski. Thalamocortical oscillations in the sleeping and aroused brain. Science, 262 (1993), pp. 679–685
51. M Steriade, D Contreras, F Amzica. Synchronized sleep oscillations and their paroxysmal developments. Trends Neurosci., 17 (1994), pp. 199–208
52. M Steriade, F Amzica, D Contreras. Synchronization of fast (30–40 Hz) spontaneous cortical rhythms during brain activation. J. Neurosci., 16 (1996), pp. 392–417
53. D.J Surmeier, A.L Towe. Properties of proprioceptive neurons in the cuneate nucleus of the cat. J. Neurophysiol., 57 (1987), pp. 938–961
54. A.L Towe, S.J Jabbur. Cortical inhibition of neurons in dorsal column nuclei of cat. J. Neurophysiol., 24 (1961), pp. 488–498
55. M Ueki, G Mies, K.A Hossmann. Effect of alpha-chloralose, halothane, pentobarbital and nitrous oxide anesthesia on metabolic coupling in somatosensory cortex of rat. Acta anaesth. scand., 36 (1992), pp. 318–322
56. J.G Valtschanoff, R.J Weinberg, A Rustioni, H.H.H.W Schmidt. Colocalization of neuronal nitric oxide synthase with GABA in rat cuneate nucleus. J. Neurocytol., 24 (1995), pp. 237–245
57. F Walberg. The fine structure of the cuneate nucleus in normal cats and following interruption of afferent fibres. An electron microscopical study with particular reference to findings made in Glees and Nauta sections. Expl Brain Res., 2 (1966), pp. 107–128